arXiv:cond-mat/0611512v1 [cond-mat.other] 20 Nov 2006

A class of permanent magnetic lattices for ultracold atoms

Saeed Ghanbari, Tien D Kieu and Peter Hannaford
Centre for Atom Optics and Ultrafast Spectroscopy
and ARC Centre of Excellence for Quantum Atom Optics,
Swinburne University of Technology, Melbourne, Australia 3122

Abstract. We report on a class of configurations of permanent magnets on an atom chip for producing 1D and 2D periodic arrays of magnetic microtraps with non-zero potential minima and variable barrier height for trapping and manipulating ultracold atoms and quantum degenerate gases. We present analytical expressions for the relevant physical quantities and compare them with our numerical results and with some previous numerical calculations. In one of the configurations of permanent magnets, we show how it is possible by changing the angle between the crossed periodic arrays of magnets to go from a 1D array of 2D microtraps to a 2D array of 3D microtraps and thus to continuously vary the barrier heights between the microtraps. This suggests the possibility of performing a type of 'mechanical' BEC to Mott insulator quantum phase transition in a magnetic lattice. We also discuss a configuration of magnets which could realize a two-qubit quantum gate in a magnetic lattice.

1. Introduction

Magnetic lattices consisting of periodic arrays of current-carrying wires [1, 2] or permanent magnetic films [3, 4] have recently been proposed as an alternative approach to optical lattices [5, 6] for trapping and manipulating small clouds of ultracold atoms and quantum degenerate gases, including Bose-Einstein condensates. Magnetic lattices may be considered as complementary to optical lattices, in much the same way as magnetic traps are complementary to optical dipole traps: they do not require (intense and stable) laser beams and there is no decoherence or light scattering due to spontaneous emission; they can produce highly stable and reproducible potential wells leading to high trap frequencies; and only atoms in low magnetic field seeking states are trapped, thus allowing the possibility of performing rf evaporative cooling *in situ* in the lattice and the study of very low temperature phenomena in a periodic lattice. Simple 1D magnetic lattices consisting of periodic arrays of traps or waveguides have been constructed using both current carrying wires [7, 8] and permanent magnets [9, 10, 11, 12] on atom chips.

In a recent paper, we proposed a 2D magnetic lattice consisting of two crossed layers of periodic arrays of parallel rectangular magnets [4]. In this paper, we report on a new class of configurations of permanent magnets comprising *four* periodic arrays of square magnets of different thickness for producing 1D and 2D arrays of magnetic microtraps with non-zero potential minima and variable barrier height. Analytical expressions are presented for various physical quantities and compared with numerical calculations. In one of the configurations of magnets, we show that by varying the angle between the crossed arrays of magnets it is possible to go from a 1D array of microtraps to a 2D array of microtraps. The 2D magnetic lattices consisting of four periodic arrays of square magnets of different thickness reported here may prove easier to implement experimentally than the crossed periodic arrays of parallel rectangular magnets proposed previously [4].

2. Periodic arrays of square permanent magnets with bias magnetic fields

Figure 1(a)-(b) shows a configuration of four periodic arrays of square magnetic slabs with thicknesses t_1, t_2, t_3 and t_4, respectively. In section 2.1, we find the components of the magnetic field due to a single array of square magnetic slabs and then use our results to obtain the total magnetic field due to the four arrays of square magnetic slabs and an external bias field $\mathbf{B_1} = B_{1x}\hat{x} + B_{1y}\hat{y}$.

2.1. Single periodic array of square magnets

Here, we consider a single infinite periodic array of square magnetic slabs of thickness t, at a distance s from the plane $z = 0$, with periodicity a along the x- and y-directions and perpendicular magnetization M_z [figure 1(c)]. The sum of this configuration and a similar one displaced by $a/2$ along the x-axis gives an infinite periodic array of parallel rectangular magnets with periodicity a along the y-direction and the same magnetization M_z and thickness t [figure 1(d)]. For distances from the surface which are large compared with $a/2\pi$, the components of the magnetic field are [4]

$$B_x = 0 \tag{1a}$$

$$B_y = B_{0y}\sin(ky)\mathrm{e}^{-kz} \tag{1b}$$

$$B_z = B_{0y}\cos(ky)\mathrm{e}^{-kz} \tag{1c}$$

where $B_{0y} = B_0(\mathrm{e}^{kt} - 1)\mathrm{e}^{ks}$, $k = 2\pi/a$ and $B_0 = 4M_z$ (Gaussian units). Considering the corresponding surface currents around the magnetic slabs in figure 1(d), we find that the array of blue (grey in grey style) square magnets produces the same component of magnetic field along the y-axis as the array of red (black in grey style) magnets. Thus, the y-component for the array of blue (or red) magnets can be written as half that of (1b). Furthermore, figure 1(c) is symmetrical with respect to x and y, and therefore, for this infinite array of square magnets, the dependence of the x-component of the magnetic field on x is the same as the dependence of the y-component of the magnetic field on y. On the other hand, the z-component of the magnetic field should be symmetrical with

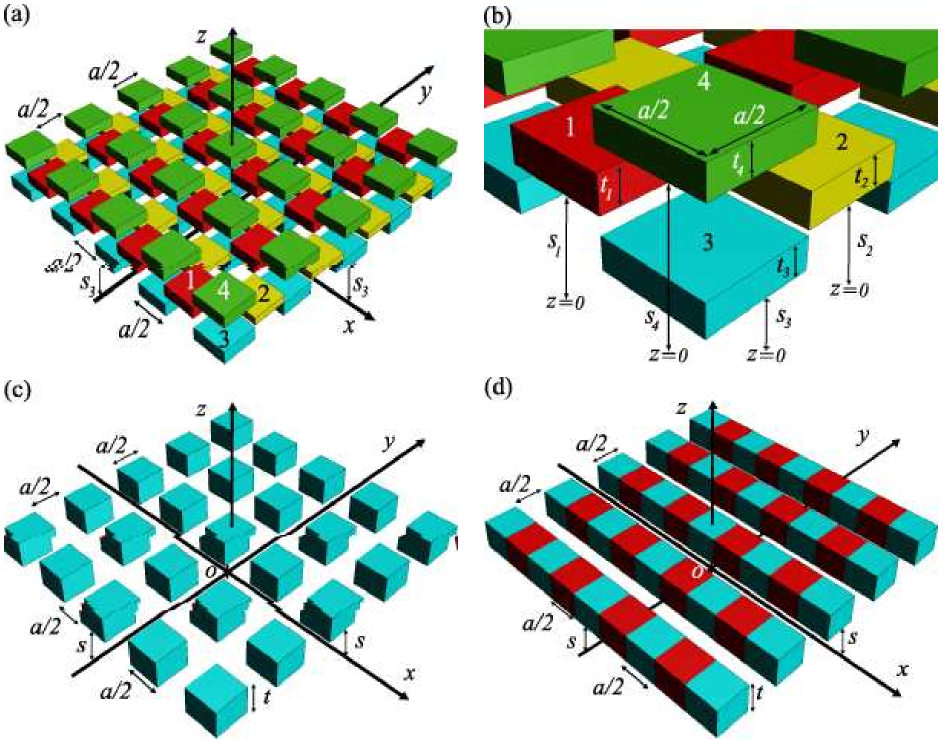

Figure 1. (a) and (b) Four periodic arrays of square permanent magnets with thicknesses t_1, t_2, t_3 and t_4, respectively. (c) Array of square permanent magnets of thickness t, at a distance s from the plane $z = 0$, with periodicity a along the x- and y-directions and perpendicular magnetization M_z. (d) Single periodic array of parallel, rectangular magnets with perpendicular magnetization.

respect to x and y and also needs to be maximum at $x = y = 0$. Thus the components of the magnetic field for the configuration of magnets in figure 1(c) may be written as

$$B_x = B_{01}\sin(kx)\mathrm{e}^{-kz} \tag{2a}$$

$$B_y = B_{01}\sin(ky)\mathrm{e}^{-kz} \tag{2b}$$

$$B_z = B_{01}[\cos(kx) + \cos(ky)]\mathrm{e}^{-kz} \tag{2c}$$

where $z \gg \frac{a}{2\pi} + s + t$ and $B_{01} = \frac{B_0}{2}(\mathrm{e}^{kt} - 1)\mathrm{e}^{ks}$.

2.2. Four periodic arrays of square magnets

Using (2a)-(2c), we can write the components of the magnetic field due to the four arrays of square permanent magnetic slabs [figure 1(a)-(b)] with external bias field $\mathbf{B_1} = B_{1x}\hat{x} + B_{1y}\hat{y}$ as

$$B_x = B_{0x}\sin(kx)\mathrm{e}^{-kz} + B_{1x} \tag{3a}$$

$$B_y = B_{0y}\sin(ky)\mathrm{e}^{-kz} + B_{1y} \tag{3b}$$

$$B_z = [B_{0x}\cos(kx) + B_{0y}\cos(ky)]\mathrm{e}^{-kz} \tag{3c}$$

where $z \gg \frac{a}{2\pi} + max(s_1 + t_1, s_2 + t_2, s_3 + t_3, s_4 + t_4)$ and

$$B_{0x} = -B_{01} + B_{02} + B_{03} + B_{04} \tag{4a}$$

$$B_{0y} = B_{01} - B_{02} + B_{03} + B_{04} \tag{4b}$$

$$B_{0i} = \frac{B_0}{2}(\mathrm{e}^{kt_i} - 1)\mathrm{e}^{ks_i}, \qquad (i = 1, 2, 3, 4) \tag{4c}$$

The magnitude of the magnetic field above the magnetic arrays is then

$$\begin{aligned} B(x, y, z) = \Big\{ & B_{1x}^2 + B_{1y}^2 \\ & + 2[B_{0x}B_{1x}\sin(kx) + B_{0y}B_{1y}\sin(ky)]\mathrm{e}^{-kz} \\ & + [B_{0x}^2 + B_{0y}^2 + 2B_{0x}B_{0y}\cos(kx)\cos(ky)]\mathrm{e}^{-2kz}\Big\}^{\frac{1}{2}} \end{aligned} \tag{5}$$

This configuration of square magnets gives a 2D periodic lattice of magnetic traps with *non-zero* potential minima given by

$$B_{min} = \frac{|B_{0x}B_{1y} - B_{0y}B_{1x}|}{(B_{0x}^2 + B_{0y}^2)^{\frac{1}{2}}} \tag{6}$$

which are located at

$$x_{min} = \left(n_x + \frac{1}{4}\right)a, \qquad n_x = 0, \pm 1, \pm 2, \cdots \tag{7a}$$

$$y_{min} = \left(n_y + \frac{1}{4}\right)a, \qquad n_y = 0, \pm 1, \pm 2, \cdots \tag{7b}$$

$$z_{min} = \frac{a}{2\pi}\ln\left(\frac{B_{0x}^2 + B_{0y}^2}{-B_{0x}B_{1x} - B_{0y}B_{1y}}\right) \tag{7c}$$

If we require a 2D lattice with *non-zero* magnetic field minima, (6) and (7c) impose the constraints

$$B_{0x}B_{1y} \neq B_{0y}B_{1x} \tag{8a}$$

$$B_{0x}^2 + B_{0y}^2 > -B_{0x}B_{1x} - B_{0y}B_{1y} > 0 \tag{8b}$$

on the geometrical parameters and the components of the bias magnetic field, where according to (4a)-(4c), B_{0x} and B_{0y} are independent of the magnetization and depend only on the geometrical constants $t_1, t_2, t_3, t_4, s_1, s_2, s_3$ and s_4.

The potential barrier heights in the three directions are given by

$$\Delta B^{x_j} = \left[\frac{4B_{0x_j}^2 B_{1x_j}^2 + (B_{0x}B_{1y} + B_{0y}B_{1x})^2}{B_{0x}^2 + B_{0y}^2}\right]^{\frac{1}{2}} - B_{min}, \; j = 1, 2 \tag{9a}$$

$$\Delta B^z = (B_{1x}^2 + B_{1y}^2)^{\frac{1}{2}} - B_{min} \tag{9b}$$

where $x_1 = x$ and $x_2 = y$. Furthermore, the curvatures of the magnetic field at the centre of the traps can be written as

$$\frac{\partial^2 B}{\partial {x_j}^2} = \frac{4\pi^2}{a^2}\frac{B_{0x_j}B_{1x_j}(B_{0x}B_{1x} + B_{0y}B_{1y})}{(B_{0x}^2 + B_{0y}^2)^{\frac{1}{2}}|B_{0x}B_{1y} - B_{0y}B_{1x}|}, \quad j = 1, 2 \tag{10a}$$

$$\frac{\partial^2 B}{\partial z^2} = \frac{\partial^2 B}{\partial x^2} + \frac{\partial^2 B}{\partial y^2} \tag{10b}$$

The trap frequencies, for an atom in hyperfine state F with magnetic quantum number m_F, are given by

$$\omega_{x_j} = \frac{2\pi\gamma}{a}\left[\frac{B_{0x_j}B_{1x_j}(B_{0x}B_{1x}+B_{0y}B_{1y})}{(B_{0x}^2+B_{0y}^2)^{\frac{1}{2}}|B_{0x}B_{1y}-B_{0y}B_{1x}|}\right]^{\frac{1}{2}}, \quad j=1,2 \tag{11a}$$

$$\omega_z = \sqrt{{\omega_x}^2 + {\omega_y}^2} \tag{11b}$$

where $\gamma = \sqrt{m_{_F} g_{_F} \mu_{_B}/m}$, $g_{_F}$ is the Landé g-factor, $\mu_{_B}$ is the Bohr magneton and m is the atomic mass.

2.2.1. Symmetrical 2D magnetic lattice To create a 2D lattice that is symmetrical with respect to x and y we impose the constraint $\Delta B^x = \Delta B^y$ from which we obtain $B_{1y} = \alpha_0 B_{1x}$, where $\alpha_0 = B_{0x}/B_{0y}$, $B_{0x} \neq 0$ and $B_{0y} \neq 0$. This is the same as the condition given in [4] for two crossed layers of infinite periodic arrays of magnets with bias fields (figure 2 (a) of [4]); so our results are the same as the equations given in [4]. Here again, our analytical expressions for B_{min}, z_{min}, ΔB^x, ΔB^y, ΔB^z, $\frac{\partial^2 B}{\partial x^2}$, $\frac{\partial^2 B}{\partial y^2}$, $\frac{\partial^2 B}{\partial z^2}$, ω_x, ω_y and ω_z depend on the x-component of the bias field B_{1x} only, rather than on both B_{1x} and B_{1y}:

$$B_{min} = \alpha_1 |B_{1x}| \tag{12a}$$

$$z_{min} = \frac{a}{2\pi}\ln\left(\frac{\alpha_2 B_{0x}}{|B_{1x}|}\right) \tag{12b}$$

$$\frac{\partial^2 B}{\partial x^2} = \frac{\partial^2 B}{\partial y^2} = \frac{1}{2}\frac{\partial^2 B}{\partial z^2} = \frac{4\pi^2\alpha_3}{a^2}|B_{1x}| \tag{12c}$$

$$\omega_x = \omega_y = \frac{\omega_z}{\sqrt{2}} = \frac{2\pi\gamma}{a}\sqrt{\alpha_3 B_{1x}} \tag{12d}$$

$$\Delta B^x = \Delta B^y = \alpha_4 |B_{1x}| \tag{12e}$$

$$\Delta B^z = \alpha_5 |B_{1x}| \tag{12f}$$

where B_{0x} and B_{0y} are given by (4a) and (4b) and $\alpha_1, \cdots, \alpha_5$ are dimensionless constants which depend on α_0 and are given by

$$\alpha_1 = \frac{|1-\alpha_0^2|}{(1+\alpha_0^2)^{\frac{1}{2}}} \tag{13a}$$

$$\alpha_2 = \frac{1}{2}\left(1+\frac{1}{\alpha_0^2}\right) \tag{13b}$$

$$\alpha_3 = \frac{2\alpha_0^2}{(1+\alpha_0^2)^{\frac{1}{2}}|1-\alpha_0^2|} \tag{13c}$$

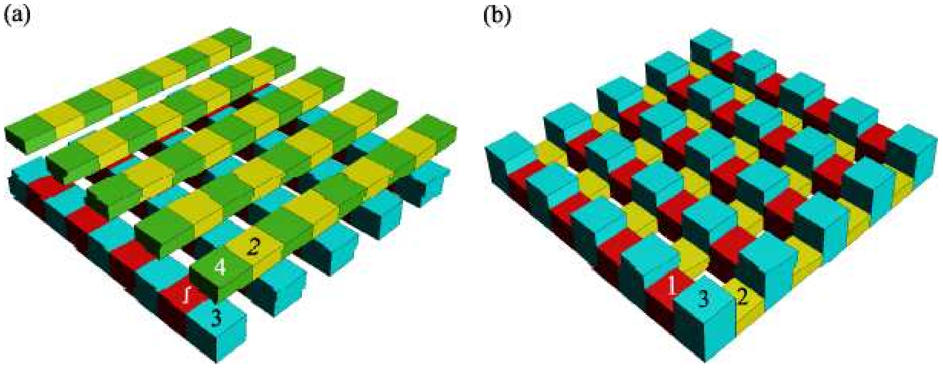

Figure 2. (a) Two crossed arrays of parallel rectangular magnets with perpendicular magnetization. (b) Three arrays of square magnets with different thickness.

$$\alpha_4 = \left(1 + \alpha_0^2 + \frac{4\alpha_0^2}{1 + \alpha_0^2}\right)^{\frac{1}{2}} - \frac{|1 - \alpha_0^2|}{(1 + \alpha_0^2)^{\frac{1}{2}}} \tag{13d}$$

$$\alpha_5 = (1 + \alpha_0^2)^{\frac{1}{2}} - \frac{|1 - \alpha_0^2|}{(1 + \alpha_0^2)^{\frac{1}{2}}} \tag{13e}$$

For a symmetrical 2D magnetic lattice with non-zero potential minima above the surface of the top array, we have the constraints which are the same as in [4]

$$\alpha_2 B_{0x} > |B_{1x}| > 0, \qquad \alpha_0 \alpha_2 B_{0y} > |B_{1y}| > 0 \tag{14a}$$

$$B_{0x} \neq B_{0y} \tag{14b}$$

2.3. *Special cases of magnetic lattices*

In this section, we consider special cases of the magnetic lattices introduced in section 2.2.

2.3.1. Single infinite periodic array of rectangular magnets When $s_3 = s_1 = 0$, $t_3 = t_1 = t$ and $t_4 = t_2 = 0$ [figure 1 (d)], we obtain an infinite periodic array of rectangular magnets and (4a)-(4c) give

$$B_{0x} = 0, \qquad B_{0y} = B_0(\mathrm{e}^{kt} - 1) \tag{15}$$

Substituting B_{0x} and B_{0y} from (15) into (5)-(11b), we obtain expressions for B_{min}, z_{min}, ΔB^x, ΔB^y, ΔB^z, $\frac{\partial^2 B}{\partial x^2}$, $\frac{\partial^2 B}{\partial y^2}$, $\frac{\partial^2 B}{\partial z^2}$, ω_x, ω_y and ω_z which are the same as in [4].

2.3.2. Two crossed arrays of parallel rectangular magnets Here, we consider a configuration of square magnets in which $t_3 = t_1$, $t_4 = t_2$, $s_2 = s_1 = 0$ and $s_4 = s_2 = s + t_1$ [figure 2(a)]. From (4a)-(4c), we have

$$B_{0x} = B_0(\mathrm{e}^{kt_2} - 1)\mathrm{e}^{k(t_1+s)}, \qquad B_{0y} = B_0(\mathrm{e}^{kt_1} - 1) \tag{16}$$

Equation (16) is in agreement with the expressions given in [4] where this magnetic lattice has been studied in detail.

2.3.3. Three arrays of square magnets with different thickness When $s_1 = s_2 = s_3 = t_4 = 0$ [figure 2(b)], from (4a)-(4c), we have

$$B_{0x} = \frac{B_0}{2}(-\mathrm{e}^{kt_1} + \mathrm{e}^{kt_2} + \mathrm{e}^{kt_3} - 1), \quad B_{0y} = \frac{B_0}{2}(\mathrm{e}^{kt_1} - \mathrm{e}^{kt_2} + \mathrm{e}^{kt_3} - 1) \tag{17}$$

We note that, according to (14b), for a symmetrical 2D lattice with non-zero magnetic potential minima, we should have $t_2 \neq t_1$. Using equations (5)-(11b) and (17) we can determine analytically the relevant quantities for this system. This magnetic lattice has already been studied numerically [4]. Table 1 gives the numerical [4] and analytical inputs and table 2 gives calculated values for the relevant quantities. There is good agreement between the analytical results for an infinite lattice and the numerical results [4] which were obtained in the central region of the lattice.

2.3.4. Chessboard configuration of square magnets In figure 2(b), if we take $t_1 = t_2$ and $t_3 = 0$, we have a chessboard configuration of square magnetic slabs. In this case, from (17), we obtain

$$B_{0x} = B_{0y} = 0 \tag{18}$$

Considering (14b), we do not have a lattice of *non-zero* magnetic field minima. In fact, we do not have a magnetic lattice, because according to (3a)-(3c) we obtain a uniform magnetic field if we look at points sufficiently far from the surface of the array.

Table 1. Numerical [4] and analytical input parameters for a configuration consisting of three arrays of square magnets with different thickness [figure 2 (b)]

Parameter	Definition	Numerical inputs	Analytical inputs
n_{sq}	Number of squares in x- or y-direction	401	∞
a (μm)	Period of magnetic lattice	1.000	1.000
$l_x = l_y$ (μm)	Length of the chip along x or y	200.5	∞
t_1 (μm)	Thickness of magnetic film (first)	0.120	0.120
t_2 (μm)	Thickness of magnetic film (second)	0.100	0.100
t_3 (μm)	Thickness of magnetic film (third)	0.220	0.220
$4\pi M_z$ (G)	Magnetization along z	3800	3800
B_{1x} (G)	Bias magnetic field along x	-5.00	-5.00
B_{1y} (G)	Bias magnetic field along y	-4.22	-4.22
B_{1z} (G)	Bias magnetic field along z	-1.87	0

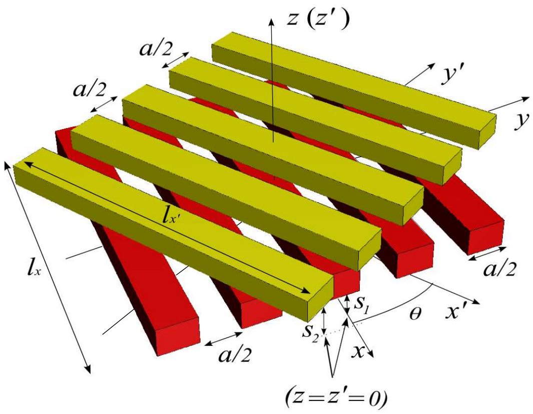

Figure 3. Two crossed arrays of parallel rectangular magnets at an arbitrary angle θ with respect to each other.

Table 2. Numerical [4] and analytical results for the input parameters from table 1 for a configuration consisting of three arrays of square magnets with different thickness [figure 2 (b)]

Parameter	Definition	Numerical results	Analytical results
x_{min} (μm)	x co-ordinate of potential minimum	0.250	0.250
y_{min} (μm)	y co-ordinate of potential minimum	0.250	0.250
z_{min} (μm)	z co-ordinate of potential minimum	0.952	0.952
d (μm)	Distance of potential minimum from surface	0.732	0.732
B_{min} (G)	Magnetic field at potential minimum	1.10	1.10
$\frac{\partial^2 B}{\partial x^2}$ ($\frac{G}{cm^2}$)	Curvature of B along x	7.52×10^{10}	7.52×10^{10}
$\frac{\partial^2 B}{\partial y^2}$ ($\frac{G}{cm^2}$)	Curvature of B along y	7.52×10^{10}	7.52×10^{10}
$\frac{\partial^2 B}{\partial z^2}$ ($\frac{G}{cm^2}$)	Curvature of B along z	1.50×10^{11}	1.50×10^{11}
ΔB^x (G)	Magnetic barrier height along x	8.10	8.10
ΔB^y (G)	Magnetic barrier height along y	8.09	8.10
ΔB^z (G)	Magnetic barrier height along z	5.45	5.45
U_{min}/k_B (μK)	Potential energy minimum	74	73
$\Delta U^x/k_B$ (μK)	Potential barrier height along x	544	544
$\Delta U^y/k_B$ (μK)	Potential barrier height along y	544	544
$\Delta U^z/k_B$ (μK)	Potential barrier height along z	366	366
$\omega_x/2\pi$ (kHz)	Trap frequency along x	350	350
$\omega_y/2\pi$ (kHz)	Trap frequency along y	350	350
$\omega_z/2\pi$ (kHz)	Trap frequency along z	494	495
$\hbar\omega_x/k_B$ (μK)	Level spacing along x	17	17
$\hbar\omega_y/k_B$ (μK)	Level spacing along y	17	17
$\hbar\omega_z/k_B$ (μK)	Level spacing along z	24	24

3. Two crossed periodic arrays of parallel rectangular magnets at an arbitrary angle with respect to each other

3.1. General case

Here, we consider a configuration of magnets which is a generalization of section 2.3.2. Figure 3 shows this configuration of rectangular magnetic slabs in which the upper array of parallel magnets is rotated at an arbitrary angle θ about the z axis which is normal to the surface. The magnets in the lower array are parallel to the x-axis while the magnets in the upper array are parallel to the x'-axis. If $\theta = \pi/2$, according to figure 3, we have the two crossed infinite periodic arrays of magnets shown in figure 2 (a). Considering the symmetry, in the rotated coordinate system of reference, we have for the upper array

$$B_{x'} = 0 \tag{19a}$$

$$B_{y'} = B_{0y'} \sin(ky')\mathrm{e}^{-kz'} \tag{19b}$$

$$B_{z'} = B_{0y'} \cos(ky')\mathrm{e}^{-kz'} \tag{19c}$$

where $B_{0y'} = B_0(\mathrm{e}^{kt_2} - 1)\mathrm{e}^{ks_2}$, $y' = -x\sin\theta + y\cos\theta$ and $z' = z$. Now, we can write the components of the magnetic field in the original coordinate system

$$B_x = B_{0y'} \sin\theta \sin(ky')\mathrm{e}^{-kz} \tag{20a}$$

$$B_y = B_{0y'} \cos\theta \sin(ky')\mathrm{e}^{-kz} \tag{20b}$$

$$B_z = B_{0y'} \cos(ky')\mathrm{e}^{-kz} \tag{20c}$$

The components of the total magnetic field due to both arrays of parallel magnets plus a bias field $\mathbf{B_1} = B_{1x}\hat{x} + B_{1y}\hat{y}$ are then

$$B_x = -B_{0y'} \sin\theta \sin(ky')\mathrm{e}^{-kz} + B_{1x} \tag{21a}$$

$$B_y = [B_{0y'} \cos\theta \sin(ky') + B_{0y} \sin(ky)]\mathrm{e}^{-kz} + B_{1y} \tag{21b}$$

$$B_z = [B_{0y'} \cos(ky') + B_{0y} \cos(ky)]\mathrm{e}^{-kz} \tag{21c}$$

where $z \gg \frac{a}{2\pi} + s_2 + t_2$ and $B_{0y} = B_0(\mathrm{e}^{kt_1} - 1)\mathrm{e}^{ks_1}$. The magnitude of the magnetic field is then

$$\begin{aligned} B(x, y, z) = \Big\{ & B_{1x}^2 + B_{1y}^2 + 2[B_{0y'}(-B_{1x}\sin\theta \\ & + B_{1y}\cos\theta)\sin(ky') + B_{0y}B_{1y}\sin(ky)]\mathrm{e}^{-kz} \\ & + (B_{0y'}^2 + B_{0y}^2 + 2B_{0y'}B_{0y}[\cos(ky')\cos(ky) \\ & + \sin(ky')\sin(ky)\cos\theta])\mathrm{e}^{-2kz}\Big\}^{\frac{1}{2}} \end{aligned} \tag{22}$$

If $\theta > 0$, these arrays of rectangular magnets can give a 2D periodic lattice of magnetic traps with *non-zero* potential minima given by

$$B_{min} = \frac{|-B_{0y}B_{1x} + B_{0y'}B_{1x}\cos\theta + B_{0y'}B_{1y}\sin^2\theta|}{(B_{0y'}^2 + B_{0y}^2 - 2B_{0y'}B_{0y}\cos\theta)^{\frac{1}{2}}} \tag{23}$$

The potential minima are located at

$$x_{min} = \left(n_x + \frac{1}{4}\right)\frac{a\sin\theta}{1-\cos\theta}, \qquad n_x = 0, \pm1, \pm2, \cdots \tag{24a}$$

$$y_{min} = \left(n_y + \frac{1}{4}\right)a, \qquad n_y = 0, \pm1, \pm2, \cdots \tag{24b}$$

$$z_{min} = \frac{a}{2\pi}\ln\left(\frac{B_{0y'}^2 + B_{0y}^2 - 2B_{0y'}B_{0y}\cos\theta}{-B_{0y'}B_{1x}\sin\theta + B_{0y'}B_{1y}\cos\theta - B_{0y}B_{1y}}\right) \tag{24c}$$

$$x'_{min} = \left(n_{x'} + \frac{1}{4}\right)\frac{a\sin\theta}{1-\cos\theta}, \qquad n_{x'} = 0, \pm1, \pm2, \cdots \tag{24d}$$

$$y'_{min} = \left(n_{y'} - \frac{1}{4}\right)a, \qquad n_{y'} = 0, \pm1, \pm2, \cdots \tag{24e}$$

The period p of the magnetic potential minima, which are located along straight lines parallel to the x- and x'-axes (defined in figure 3), varies with θ and is given by

$$p = \left|\frac{a\sin\theta}{1-\cos\theta}\right| \tag{25}$$

If θ changes between 0 and $\pi/2$, the period of the magnetic lattice varies between ∞ and the minimum period a, which is the period of the magnetic slabs along the y- and y'-axes. Now, we can write the constraints for a lattice with *non-zero* magnetic field minima

$$-B_{0y}B_{1x} + B_{0y'}B_{1x}\cos\theta + B_{0y'}B_{1y}\sin^2\theta \neq 0 \tag{26a}$$

$$B_{0y'}^2 + B_{0y}^2 - 2B_{0y'}B_{0y}\cos\theta > -B_{0y'}B_{1x}\sin\theta + B_{0y'}B_{1y}\cos\theta - B_{0y}B_{1y} > 0 \tag{26b}$$

According to (23)-(24c) and the contour plots of the magnetic field for different values of θ (figure 4), apart from $\theta = 0$ for which we have a 1D array of 2D magnetic microtraps, we have a 2D array of 3D microtraps with different periods in the x- and x'-directions, as θ varies. Looking at figure 4 more carefully, we find that as θ changes the distance between the magnetic traps along the interior bisector of the angle θ between the positive y- and y'-axes also changes. Thus, depending on the barrier heights, the tunnelling rate between the traps in this direction will be higher than the tunnelling rate in the x- and x'-directions. Here, we give the barrier heights in the x-, x'- and z-directions

$$\Delta B^{x_j} = \left\{\left[B_{1x} - (-1)^j\frac{B_{0y'}\sin\theta(B_{0y}B_{1y} - B_{0y'}B_{1y}\cos\theta + B_{0y'}B_{1x}\sin\theta)}{B_{0y'}^2 + B_{0y}^2 - 2B_{0y'}B_{0y}\cos\theta}\right]^2 \right.$$
$$\left. + \left[B_{1y} + (-1)^j\frac{(B_{0y} + B_{0y'}\cos\theta)(B_{0y}B_{1y} - B_{0y'}B_{1y}\cos\theta + B_{0y'}B_{1x}\sin\theta)}{B_{0y'}^2 + B_{0y}^2 - 2B_{0y'}B_{0y}\cos\theta}\right]^2\right\}^{\frac{1}{2}}$$
$$- B_{min}, \qquad j = 1 \text{ or } 4 \tag{27a}$$

$$\Delta B^z = (B_{1x}^2 + B_{1y}^2)^{\frac{1}{2}} - B_{min} \tag{27b}$$

where, $x_1 = x$, $x_4 = x'$ and by definition we have

$$\Delta B^x = B(x = x_{max}, y = y_{min}, z_{min}) - B_{min} \tag{28a}$$

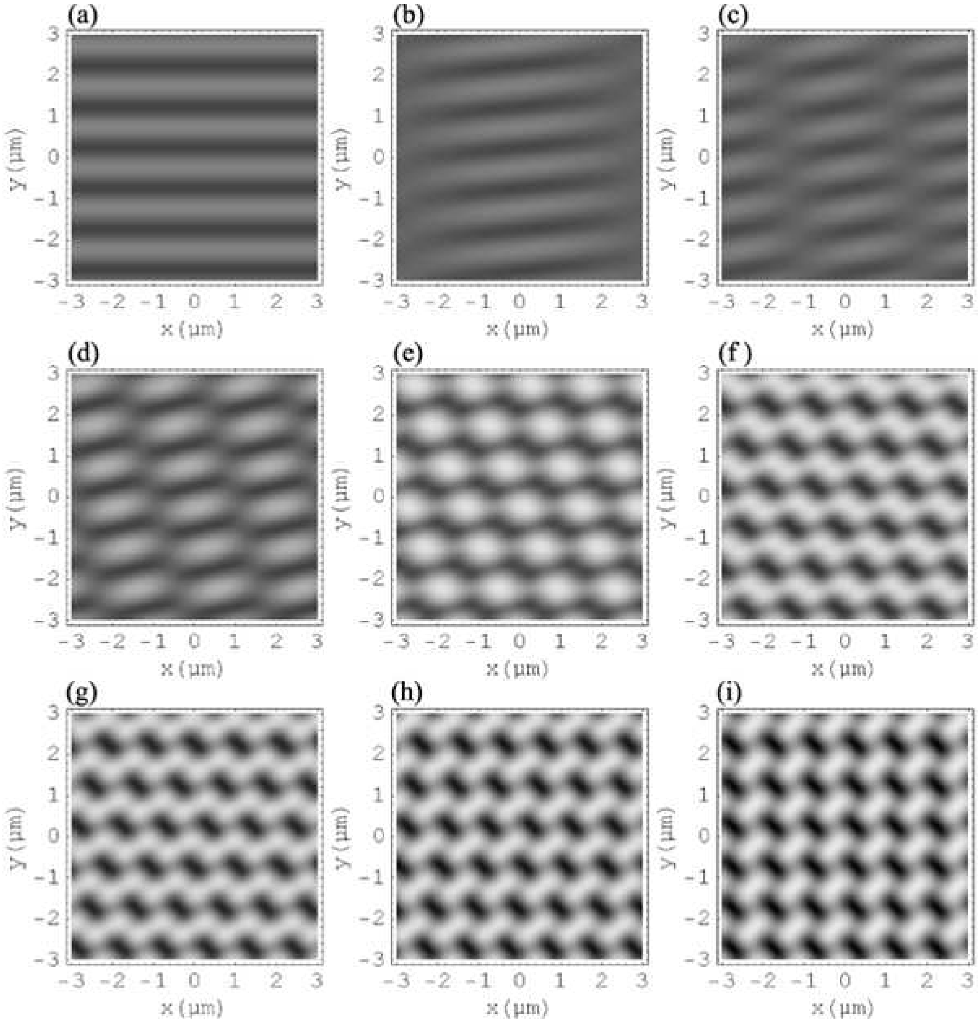

Figure 4. Density plot of the magnetic field, calculated using analytical expressions, for two crossed arrays of parallel rectangular magnets at an arbitrary angle θ with respect to each other for the input parameters from table 3 and (a) $\theta = 0$ (b) $\theta = \pi/18$ (c) $\theta = \pi/9$ (d) $\theta = \pi/6$ (e) $\theta = \pi/4$ (f) $\theta = \pi/3$ (g) $\theta = 7\pi/18$ (h) $\theta = 4\pi/9$ (i) $\theta = \pi/2$

.

$$\Delta B^{x'} = B(x = x'_{max}, y = y'_{min}, z_{min}) - B_{min} \qquad (28b)$$

$$\Delta B^{z} = B(x_{min}, y_{min}, z = \infty) - B_{min} \qquad (28c)$$

where

$$x_{max} = \frac{a \sin\theta}{1-\cos\theta}\left(n_x + \frac{3}{4}\right), \qquad n_x = 0, \pm 1, \pm 2, \cdots \qquad (29a)$$

$$x'_{max} = \frac{a \sin\theta}{1-\cos\theta}\left(n_{x'} + \frac{3}{4}\right), \qquad n_{x'} = 0, \pm 1, \pm 2, \cdots \qquad (29b)$$

We also have

$$\Delta B^{x} = B(y' = \frac{a}{4}, y = \frac{a}{4}, z_{min}) - B_{min} \qquad (30a)$$

$$\Delta B^{x'} = B(y' = -\frac{3a}{4}, y = \frac{a}{4}, z_{min}) - B_{min} \tag{30b}$$

Furthermore, the curvatures are given by

$$\begin{aligned}\frac{\partial^2 B}{\partial x^2} = {} & \frac{\pi^2}{a^2 F^{\frac{3}{2}} G} B_{0y'} \sin^2\theta [2B_{0y'}(B_{0y'}^2 + B_{0y}^2)(B_{1x}^2 + B_{1y}^2) \\ & - B_{0y} B_{0y'}^2 (B_{1x}^2 + 7B_{1y}^2)\cos\theta - 2B_{0y'}(B_{0y'}^2 + B_{0y}^2)(B_{1x}^2 - B_{1y}^2)\cos 2\theta \\ & + B_{0y} B_{0y'}^2 (B_{1x}^2 - B_{1y}^2)\cos 3\theta + 2B_{0y}(3B_{0y'}^2 + 2B_{0y}^2) B_{1x} B_{1y} \sin\theta \\ & - 4B_{0y'}(B_{0y'}^2 + B_{0y}^2) B_{1x} B_{1y} \sin 2\theta + 2B_{0y} B_{0y'}^2 B_{1x} B_{1y} \sin 3\theta]\end{aligned} \tag{31a}$$

$$\begin{aligned}\frac{\partial^2 B}{\partial x'^2} = {} & \frac{\pi^2}{a^2 F^{\frac{3}{2}} G} B_{0y} \sin^2\theta [B_{0y'}(-8{B_{0y}}^2 {B_{1y}}^2 + B_{0y'}^2 (B_{1x}^2 - B_{1y}^2)\cos\theta \\ & - B_{0y'}^3 (B_{1x}^2 - B_{1y}^2)\cos 3\theta + 4B_{1y}(B_{0y}(B_{0y}^2 + {B_{0y'}}^2) B_{1y} \\ & + B_{0y'} B_{1x}(B_{0y}^2 - {B_{0y'}}^2 \cos 2\theta)\sin\theta)]\end{aligned} \tag{31b}$$

$$\begin{aligned}\frac{\partial^2 B}{\partial y^2} = {} & \frac{2\pi^2}{a^2 F^{\frac{3}{2}} G} (B_{0y} B_{1y} - B_{0y'} B_{1y} \cos\theta + B_{0y'} B_{1x} \sin\theta)[\\ & (B1y(2B0y^3 + B_{0y'}\cos\theta(-6B_{0y}^2 + B_{0y'}\cos\theta(-2B_{0y'}\cos\theta \\ & + B_{0y}(5 + \cos 2\theta))))) + 2B_{0y'} B_{1x} \cos\theta (B_{0y'} - B_{0y}\cos\theta) \\ & (-B_{0y} + B_{0y'}\cos\theta)\sin\theta + 2B_{0y} B_{0y'}^2 B_{1y} \sin^2\theta]\end{aligned} \tag{31c}$$

$$\begin{aligned}\frac{\partial^2 B}{\partial y'^2} = {} & \frac{\pi^2}{a^2 F^{\frac{3}{2}} G} (B_{0y} B_{1y} - B_{0y'} B_{1y} \cos\theta + B_{0y'} B_{1x} \sin\theta)[\\ & 2B_{1y}\cos\theta(-5B_{0y}^2 B_{0y'} - 2{B_{0y'}}^3 + 2B_{0y}^3 \cos\theta + 7B_{0y}{B_{0y'}}^2 \cos\theta \\ & - B_{0y} B_{0y'}(B_{0y} + B_{0y'}\cos\theta)\cos 2\theta) + B_{0y'} B_{1x}(4({B_{0y}}^2 + {B_{0y'}}^2) \\ & + B_{0y} B_{0y'}(-9\cos\theta + \cos 3\theta))\sin\theta]\end{aligned} \tag{31d}$$

$$\frac{\partial^2 B}{\partial z^2} = \frac{4\pi^2}{a^2 F^{\frac{1}{2}} G} (B_{0y} B_{1y} - B_{0y'} B_{1y} \cos\theta + B_{0y'} B_{1x} \sin\theta)^2 \tag{31e}$$

where

$$F = |B_{0y'}^2 + B_{0y}^2 - 2B_{0y} B_{0y'} \cos\theta| \tag{32a}$$

$$G = | - B_{0y} B_{1x} + B_{0y'} B_{1x} \cos\theta + B_{0y'} B_{1y} \sin\theta| \tag{32b}$$

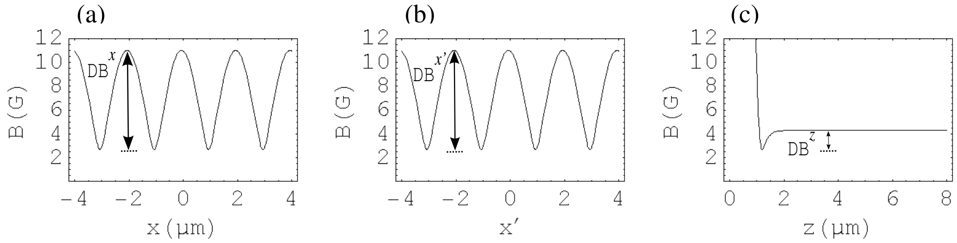

Figure 5. Magnetic field produced by two crossed arrays of parallel rectangular magnets at an angle $\theta = \pi/6$ with respect to each other, with input parameters from table 3. Curves (a)-(c) show the analytical results of the magnetic field (a) along a line ($y = y_{min}$, $z = z_{min}$) parallel to the x-axis, (b) along a line ($y' = y'_{min}$, $z = z_{min}$) parallel to the x'-axis, and (c) along a line ($x = x_{min}$, $y = y_{min}$) parallel to the z-axis.

3.2. Symmetrical lattice

For $\theta \neq 0$, if we have $B_{1y} = \beta_0(\theta)B_{1x}$, where $\beta_0(\theta) = B_{0y'}\sin\theta/(B_{0y'}\cos\theta + B_{0y})$, then the barrier heights in the x- and x'-directions are equal. Thus, we have a symmetrical 2D lattice of 3D microtraps in the x- and x'-directions and, as figure 5 shows, the microtraps in the x- and x'-directions have the same period. This figure shows our

Table 3. Numerical and analytical input parameters for two crossed arrays of parallel rectangular magnets at an angle $\theta = \pi/6$ with respect to each other (figure 3): (1) numerical inputs (2) analytical inputs

Parameter	Definition	Numerical inputs	Analytical inputs
n_r	Number of parallel rectangular magnets in x- or x'-direction	1001	∞
a (μm)	Period of magnetic lattice	1.000	1.000
$l_x = l'_x$ (μm)	Length of the magnets along x- or x'-direction	1000.5	∞
t_1 (μm)	Thickness of magnetic slabs parallel to the x-direction	0.322	0.322
t_2 (μm)	Thickness of magnetic slabs parallel to the x'-direction	0.083	0.083
s_1 (μm)	Distance from the plane $z = 0$ to the lower surface of the magnets parallel to the x-direction	0.000	0.000
s_2 (μm)	Distance from the plane $z = 0$ to the lower surface of the magnets parallel to the x'-direction	0.422	0.422
$4\pi M_z$ (G)	Magnetization along z	3800	3800
B_{1x} (G)	Bias magnetic field along x	-4.08	-4.08
B_{1y} (G)	Bias magnetic field along y	-1.32	-1.32
B_{1z} (G)	Bias magnetic field along z	-0.69	0.00

analytical results for an infinite lattice, which are in excellent agreement with our numerical calculations in the central region of the lattice. For the numerical calculations we have written a Mathematica code and have used the software package Radia [13] interfaced to Mathematica. Here, the quantities of interest are

$$B_{min} = \beta_1(\theta)|B_{1x}| \tag{33a}$$

$$z_{min} = \frac{a}{2\pi}\ln\left[\frac{\beta_2(\theta)B_{0y}}{|B_{1x}|}\right] \tag{33b}$$

$$\frac{\partial^2 B}{\partial x^2} = \frac{\partial^2 B}{\partial x'^2} = \frac{4\pi^2\beta_3(\theta)}{a^2}|B_{1x}| \tag{33c}$$

$$\frac{\partial^2 B}{\partial y^2} = \frac{\partial^2 B}{\partial y'^2} = \frac{4\pi^2\beta_4(\theta)}{a^2}|B_{1x}| \tag{33d}$$

$$\frac{\partial^2 B}{\partial z^2} = \frac{4\pi^2\beta_5(\theta)}{a^2}|B_{1x}| \tag{33e}$$

$$\omega_x = \omega_{x'} = \frac{2\pi\gamma}{a}\sqrt{\beta_3(\theta)B_{1x}} \tag{33f}$$

Table 4. Numerical and analytical results for the input parameters from table 3 for two crossed arrays of parallel rectangular magnets at an angle $\theta = \pi/6$ with respect to each other (figure 3)

Parameter	Definition	Numerical results	Analytical results
x_{min} (μm)	x co-ordinate of potential minimum	0.933	0.933
y_{min} (μm)	y co-ordinate of potential minimum	0.250	0.250
z_{min} (μm)	z co-ordinate of potential minimum	1.200	1.200
d (μm)	Distance of potential minimum from surface	0.695	0.695
B_{min} (G)	Magnetic field at potential minimum	2.68	2.68
$\frac{\partial^2 B}{\partial x^2}$ $(\frac{G}{cm^2})$	Curvature of B along x	1.05×10^{10}	1.05×10^{10}
$\frac{\partial^2 B}{\partial y^2}$ $(\frac{G}{cm^2})$	Curvature of B along y	5.99×10^9	5.98×10^9
$\frac{\partial^2 B}{\partial z^2}$ $(\frac{G}{cm^2})$	Curvature of B along z	1.65×10^{10}	1.65×10^{10}
ΔB^x (G)	Magnetic barrier height along x	8.32	8.33
$\Delta B^{x'}$ (G)	Magnetic barrier height along x'	8.31	8.33
ΔB^z (G)	Magnetic barrier height along z	1.60	1.60
U_{min}/k_B (μK)	Potential energy minimum	180	180
$\Delta U^x/k_B$ (μK)	Potential barrier height along x	559	559
$\Delta U^{x'}/k_B$ (μK)	Potential barrier height along x'	558	559
$\Delta U^z/k_B$ (μK)	Potential barrier height along z	108	108
$\omega_x/2\pi$ (kHz)	Trap frequency along x	131	131
$\omega_y/2\pi$ (kHz)	Trap frequency along y	99	99
$\omega_z/2\pi$ (kHz)	Trap frequency along z	164	164
$\hbar\omega_x/k_B$ (μK)	Level spacing along x	6	6
$\hbar\omega_y/k_B$ (μK)	Level spacing along y	5	5
$\hbar\omega_z/k_B$ (μK)	Level spacing along z	8	8

$$\omega_y = \omega_{y'} = \frac{2\pi\gamma}{a}\sqrt{\beta_4(\theta)B_{1x}} \tag{33g}$$

$$\omega_z = \frac{2\pi\gamma}{a}\sqrt{\beta_5(\theta)B_{1x}} \tag{33h}$$

$$\Delta B^x = \Delta B^{x'} = \beta_6(\theta)|B_{1x}| \tag{33i}$$

$$\Delta B^z = \beta_7(\theta)|B_{1x}| \tag{33j}$$

where $\gamma = \sqrt{m_F g_F \mu_B / m}$ and $\beta_1(\theta)$, $\cdots$, $\beta_7(\theta)$ are dimensionless parameters which depend on $c_0 = B_{0y'}/B_{0y}$ and θ. Using the definitions $c_1 = 1 - c_0^2$, $c_2 = 1 + c_0^2$, $h_1(\theta) = 1 + c_0\cos\theta$ and $h_2(\theta) = 1 + c_0^2 - 2c_0\cos\theta$, we have

$$\beta_0(\theta) = \frac{c_0\sin\theta}{h_1(\theta)} \tag{34a}$$

$$\beta_1(\theta) = \frac{|c_1|}{|h_1(\theta)|[h_2(\theta)]^{\frac{1}{2}}} \tag{34b}$$

$$\beta_2(\theta) = \frac{h_1(\theta)h_2(\theta)}{2c_0\sin\theta} \tag{34c}$$

$$\beta_3(\theta) = \frac{2c_0^2c_2\sin^4\theta}{|c_1h_1(\theta)|[h_2(\theta)]^{\frac{3}{2}}} \tag{34d}$$

$$\beta_4(\theta) = \frac{c_0^2[-8c_0\cos\theta + c_2(3+\cos 2\theta)]\sin^2\theta}{|c_1h_1(\theta)|[h_2(\theta)]^{\frac{3}{2}}} \tag{34e}$$

$$\beta_5(\theta) = \frac{4c_0^2\sin^2\theta}{|c_1h_1(\theta)|[h_2(\theta)]^{\frac{1}{2}}} \tag{34f}$$

$$\beta_6(\theta) = \frac{[c_2^3 - 2c_0c_1^2\cos\theta - 4c_0^2c_2\cos 2\theta]^{\frac{1}{2}}}{|h_1(\theta)h_2(\theta)|} - \beta_1(\theta) \tag{34g}$$

$$\beta_7(\theta) = [1 + \beta_0(\theta)^2]^{\frac{1}{2}} - \beta_1(\theta) \tag{34h}$$

Subject to $B_{1y} = \beta_0(\theta)B_{1x}$, the conditions for *non-zero* magnetic potential minima are

$$B_{0y} \neq B_{0y'} \tag{35a}$$

$$\beta_2(\theta)B_{0y} > |B_{1x}| > 0 \tag{35b}$$

According to (33*f*)-(33*h*), (34*d*) and (34*e*), for a constant c_0, it is possible to change the trap frequencies by varying θ and/or the bias magnetic field $\mathbf{B_1}$. Furthermore, as (33*i*), (33*j*), (34*g*) and (34*h*) indicate, we can adjust the magnetic field potential barriers by changing the angle θ, the bias magnetic field $\mathbf{B_1}$, or both.

Table 3 gives the numerical and analytical inputs and table 4 gives calculated values for the relevant quantities. There is good agreement between the analytical results for an infinite lattice and the numerical results which were obtained in the central region of the lattice.

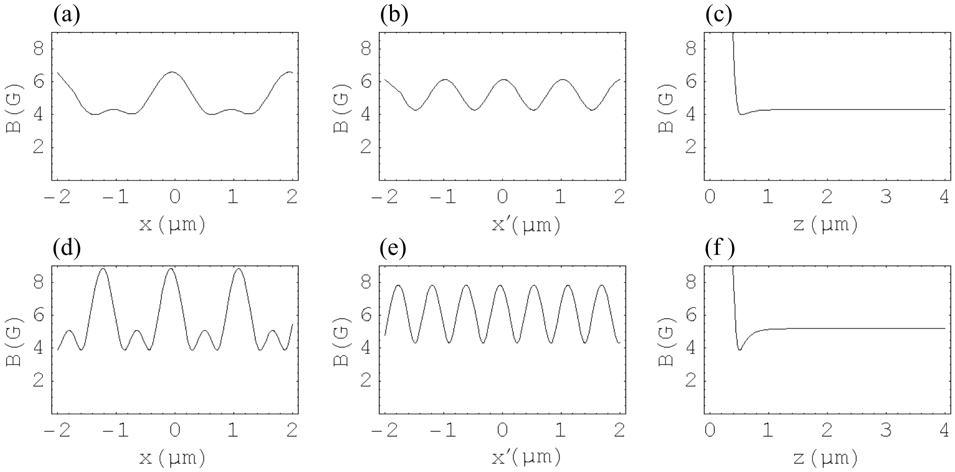

Figure 6. Magnetic field produced by three arrays of parallel rectangular magnets, as described in section 4. The parallel magnets in the middle and the top arrays have an angle with respect to the parallel magnets in the lower array of $\theta = \pi/6$ in (a)-(c) and $\theta = \pi/3$ in (d)-(f). The curves show the analytical magnetic field along a line ($y = y_{min}$, $z = z_{min}$) parallel to the x-axis, (a) and (d), along a line ($y' = y'_{min}$, $z = z_{min}$) parallel to the x'-axis, (b) and (e), and along a line ($x = x_{min}$, $y = y_{min}$) parallel to the z-axis, (c) and (f).

4. Three periodic arrays of parallel rectangular magnets

Here, we consider a special configuration involving three periodic arrays of parallel rectangular magnets. The lower array (array 1) and the middle array (array 2) are at an angle θ with respect to each other, similar to the crossed arrays shown in figure 3, while the rectangular magnets in the top array (array 3) are parallel to those of the middle array and remain parallel as θ changes. The period a_3 is twice the periods a_1 and a_2. To obtain the components of the magnetic field due to these three arrays of magnets plus bias field $\mathbf{B_1} = B_{1x}\hat{x} + B_{1y}\hat{y}$, we add the magnetic field due to array 3 to that of arrays 1 and 2 [(21a)-(21c)]:

$$B_x = -B_{0y'}\sin\theta\sin(ky')\mathrm{e}^{-kz} - B_{0y''}\sin\theta\sin(ky'/2)\mathrm{e}^{-kz/2} + B_{1x} \tag{36a}$$

$$B_y = [B_{0y'}\cos\theta\sin(ky') + B_{0y}\sin(ky)]\mathrm{e}^{-kz} + [B_{0y''}\cos\theta\sin(ky'/2)]\mathrm{e}^{-kz/2} + B_{1y} \tag{36b}$$

$$B_z = [B_{0y'}\cos(ky') + B_{0y}\cos(ky)]\mathrm{e}^{-kz} + B_{0y''}\cos(ky'/2)\mathrm{e}^{-kz/2} \tag{36c}$$

where $z \gg \frac{a}{\pi} + s_3 + t_3$ and $B_{0y} = B_0(\mathrm{e}^{kt_1} - 1)\mathrm{e}^{ks_1}$, $B_{0y'} = B_0(\mathrm{e}^{kt_2} - 1)\mathrm{e}^{ks_2}$ and $B_{0y''} = B_0(\mathrm{e}^{kt_3/2} - 1)\mathrm{e}^{ks_3/2}$. This magnetic field is shown for $\theta = \pi/6$ and $\theta = \pi/3$ in figure 6 (a)-(c) and figure 6 (d)-(f), respectively. The period $a_3 = 1$ μm, which is twice the periods a_1 and a_2. The thicknesses of the layers are $t_1 = 50$ nm, $t_2 = 40$ nm and $t_3 = 5$ nm and the lower surfaces of the layers are at distances $s_1 = 0$, $s_2 = 60$ nm and $s_3 = 105$ nm from the plane $z = 0$. The magnetization is as before and the components of the bias magnetic field are $B_{1x} = -4.08$ G, $B_{1y} = -1.39$ G and $B_{1z} = 0$. According to figure 6, we can change the separation and also the barrier height between adjacent microtraps by varying θ. This might be of interest for a two-qubit quantum gate process [14].

5. Discussion and summary

We have introduced a class of permanent magnetic lattices for ultracold atoms and quantum degenerate gases. The potential barriers between the adjacent microtraps can be altered by varying the bias magnetic field, as indicated by the relevant equations. Thus, these configurations of permanent magnets together with an adjustable bias magnetic field could be used to study quantum tunnelling and to realize a BEC to Mott insulator quantum phase transition for quantum information processing in a magnetic lattice.

We have shown that for a configuration of two crossed periodic arrays of parallel rectangular magnets with a variable angle between the two arrays, the magnetic lattice goes from a 1D to a 2D lattice as the angle θ between the arrays is changed from 0 to $\pi/2$. This may prove useful for loading ultracold atoms into a 2D lattice of 3D microtraps by initially loading the atoms into the 1D lattice of 2D microtraps and then by changing the angle from $\theta = 0$ to $\theta = \pi/2$. Also, by varying the angle θ, it is possible to change the depth of the traps adiabatically, which suggests the possibility of realizing a 'mechanical' BEC to Mott insulator quantum phase transition in a magnetic lattice. Moreover, the period of the magnetic lattice can be adjusted as the angle θ is changed. This could have applications in quantum information processing and also in creating new artificial crystalline materials. In a more general case, it is possible to have two different periods $a_y = a_1$ and $a_{y'} = a_2$ in the y- and y'-directions, respectively, to allow for a more flexible magnetic lattice. A configuration of magnets with three periodic arrays of rectangular magnets having two different periods $a_1 = a_2$ and a_3 may be useful for implementing a two-qubit quantum gate [14] in a magnetic lattice.

Acknowledgments

This project is supported by Swinburne University strategic initiative funding. Saeed Ghanbari would like to thank the Iranian Government for financial support.

References

[1] Yin J, Gao W, Hu J and Wang Y 2002 *Opt. Commun.* **206** 99
[2] Grabowski A and Pfau T 2003 *Eur. Phys. J. D* **22** 347
[3] Hinds E A and Hughes I G 1999 *J. Phys. D: Appl. Phys.* **32** R119
[4] Ghanbari S, Kieu T D, Sidorov A and Hannaford P 2006 *J. Phys. B: At. Mol. Opt. Phys.* **39** 847
[5] Jaksch D, Bruder C, Cirac J I, Gardiner C W and Zoller P 1998 *Phys. Rev. Lett.* **81** 3108
[6] Greiner M, Mandel O, Esslinger T, Hänsch T and Bloch I 2002 *Nature* **415** 39
[7] Günther A, Kraft S, Kemmler M, Koelle D, Kleiner R, Zimmermann C and Fortágh J 2005 *Phys. Rev. Lett.* **95** 170405

[8] Hänsel W, Hommelhoff P, Hänsch T W and Reichel J 2001 *Nature* **413** 498

[9] Barb I, Gerritsma R, Xing Y T, Goedkoop J B and Spreeuw R J C 2005 *Eur. Phys. J D* **35** 75

[10] Sinclair C D J, Curtis E A, Llorente-Garcia I, Retter J A, Hall B V, Eriksson S, Sauer B E and Hinds E A 2005 *Phys Rev. A* **72** 031603

[11] Sidorov A I, McLean R J, Scharnberg F, Gough D S, Davis T J, Sexton B A, Opat G I and Hannaford P 2002 *Acta Phys. Polonica B* **33** 2137

[12] Boyd M, Streed E W, Medley P, Campbell G K, Mun J, Ketterle W and Pritchard D E arXiv:cond-mat/0608370 v1 16 Aug 2006

[13] Available from: http://www.esrf.fr/machine/support/ids/public/index.html

[14] Barenco A, Bennett C H, Cleve R, Divicenzo D P, Margolus N, Shor P, Sleator T, Smolin J A and Weinfurter H 1995 *Phys Rev. A* **52** 3457